Effects of Gamma Ray Irradiation on Ejecta Size from CFRP Plates

Masahiro Nishida[(1)], Yasuyuki Hiraiwa[(2)], Koichi Hayashi[(3)], Masumi Higashide[(4)]

[(1)] Nagoya Institute of Technology, Gokiso-cho, Showa-ku, Nagoya, Aichi, 466-8555, Japan, Email: nishida.masahiro@nitech.ac.jp
[(2)] Nagoya Institute of Technology, Gokiso-cho, Showa-ku, Nagoya, Aichi, 466-8555, Japan
[(3)] National Institute of Technology, Toba College, 1-1, Ikegami-cho, Toba City, Mie, 517-8501, Japan
[(4)] Aerospace Research and Development Directorate, Japan Aerospace Exploration Agency, 7-44-1 Jindaiji Higashi-machi, Chofu-shi, Tokyo 182-8522, Japan

ABSTRACT

In this study, we examined the effects of gamma ray irradiation on fragment size from carbon fiber reinforced plastics (CFRP) plates due to hypervelocity impact. Quasi-isotropic CFRP plates consisting of unidirectional pre-preg sheets and spherical projectiles made of aluminum allow with a diameter of 1 mm (2017-T4) were used. A witness plate (200 mm × 200 mm, 2 mm in thickness) made of copper, C1100P-1/4H, with a hole of 30 mm was placed 50 mm in front of and behind each target to examine ejecta based on ISO 11227. The fragments collected from in front of and behind targets were compared. The gamma ray irradiation decreased the number of fragments and the fragment size on the rear side and did not affect the number of fragments and the fragment size on the impact side. The penetration hole of projectiles changed with the gamma ray irradiation.

1 INTRODUCTION

As is well known, because carbon fiber reinforced plastics (CFRP) plates show high specific strength and high specific stiffness, CFRP plates have been widely used in satellites and spacecraft for weight saving. However, under unforgiving space environment [1, 2] such as high-level vacuum, ultraviolet (UV) radiation, electron beam (EB) [3, 4], atomic oxygen (AO) and thermal cycling, the strength and stiffness of CFRP decrease and degradation-related studies have been studying [5].

Because of impact of micrometeoroids and orbital debris (MMOD) as one of unforgiving space environment, many studies have been conducted on the ballistic limit, fracture behavior [6, 7] and fragments [8, 9] when projectiles struck CFRP plates at over 10 km/s in addition to widely-used aluminum alloy plates. From a viewpoint of the increase in space debris, the ejecta from targets and fractured projectiles (hereinafter, referred to as fragments) are important when projectiles struck CFRP plates. The authors' group has been studying fragments when projectiles have struck CFRP plates [10] or widely-used aluminum alloy plates [11].

In this study, aluminum alloy projectiles struck gamma-ray-irradiated CFRP plates. Fragments from CFRP plates collected from test chamber were measured. The effects of gamma ray irradiation on fragments from CFRP plates were examined.

2 EXPERIMENTAL METHOD

We employed CFRP laminates consisting of epoxy-based carbon fiber UD pre-pregs (Toray, P13080F-3: Matrix 3800-2, Fiber M60JB) as a target material. The size of the CFRP laminates was 75×100 mm, with thickness of 0.7 mm, and the constitution of the CFRP laminates was [+45º/+45º/0º/0º/−45º/−45º/90º/90º]s (16 ply). CFRP plates were irradiated by gamma ray at the sixth cell of Cobalt-60 Gumma-ray Irradiation Facility, Takasaki Advanced Radiation Research Institute (TARRI), National Institutes for Quantum and Radiological Science and Technology (QST). Total doze was 0.5 MGy (1 kGy/h, 500 hours) and 10 MGy (10 kGy/h, 1000 hours). CFRP plates were encapsulated inside an evacuated glass ampoule during gamma ray irradiation.

Projectiles with a diameter of 1 mm made of aluminum alloy (2017-T4) were used based on ISO 11227. A two-stage light-gas gun at Nagoya Institute of Technology was used to accelerate the projectiles with a sabot. The impact velocity was fixed at 2.4 km/s.

Front witness plates (150 mm×150 mm) and rear witness plates (200 mm×200 mm) of 2 mm in thickness made of copper, C1100P-1/4H, were placed 50 mm in front of and behind each target as shown in Fig. 1 to determine the scattering area and examine impact craters impacted by the ejecta fragments. The front witness plates have a hole of 30 mm so that projectiles could pass through. When the forward fragments and backward fragments coming from the target were separately collected, the space between the target and the rear witness plate was surrounded by plates.

Proc. 7th European Conference on Space Debris, Darmstadt, Germany, 18–21 April 2017, published by the ESA Space Debris Office
Ed. T. Flohrer & F. Schmitz, (http://spacedebris2017.sdo.esoc.esa.int, June 2017)

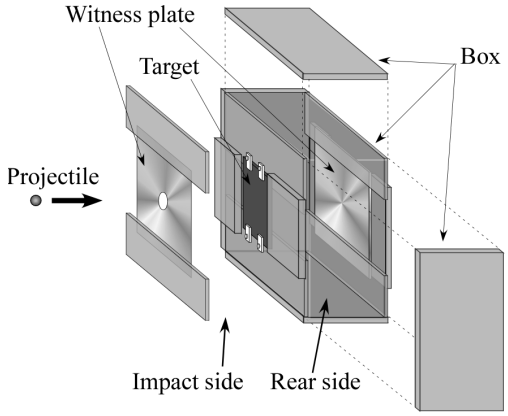

Figure 1. Experimental setup

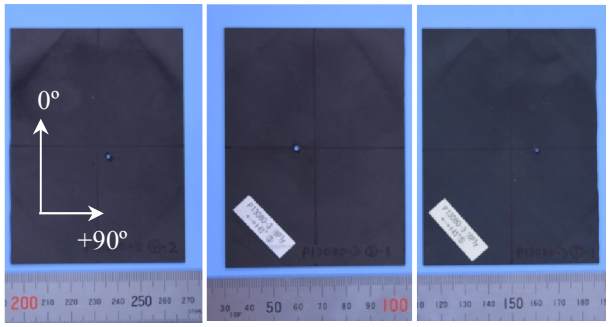

(a) No irradiation (2.41 km/s) (b) 0.5 MGy (2.38 km/s) (c) 10 MGy (2.41 km/s)

Figure 2. Impact side photographs of CFRP plates after impact experiment

3 RESULTS AND DISCUSSION

Fig. 2 shows photographs of targets after impact experiments. Fig. 3 shows enlarged images of Fig. 2. We can observe that the surface layers on the impact side were peeled off from top right to bottom left and those on the rear side were peeled off from top left to bottom right. The peeled-off areas were large. The direction from top right to bottom left on the impact side is coincident with the fiber direction of the outermost layer on the impact side. The direction on the rear side is the same as well.

Table 1 show the areas of penetration holes which were measured by image analysis of Fig. 3. The area of penetration hole of 0.5 MGy specimens was larger than that of the unirradiated specimen. The penetration hole of 0.5 MGy specimens was approximately 2 mm in diameter which is larger than the projectile diameter of 1 mm. The penetration hole of 10 MGy specimens was smaller than those of the unirradiated specimen and 0.5 MGy specimens. It was expected that strength and/or elongation of 10 MGy specimens drastically decreased by the irradiation of gamma ray.

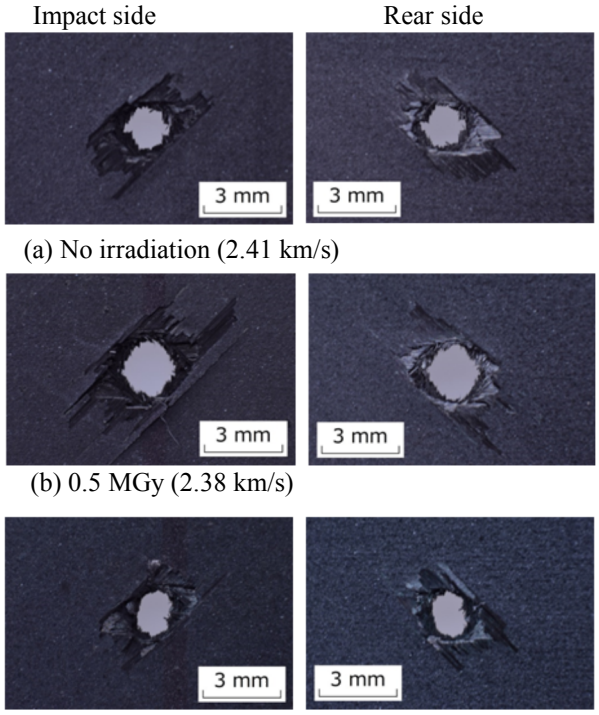

(a) No irradiation (2.41 km/s)

(b) 0.5 MGy (2.38 km/s)

(c) 10 MGy (2.41 km/s)

Figure 3. Enlarged images of Fig. 2 near penetration hole

Table 1 Areas of perforation holes

No irradiation	0.5 MGy	10 MGy
2.0 mm^2	3.1 mm^2	1.8 mm^2

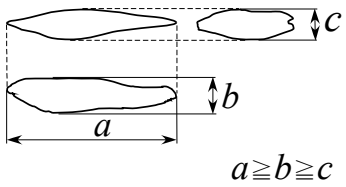

Figure 4. Definition of fragments collected from test chamber

After impact experiments, size of fragments collected from test chamber were measured using image analysis software (ImageJ). The length, *a*, width, *b*, and thickness, *c*, of fragments was defined as shown in Fig. 4.

Figs. 5(a) and (d) show the cumulative number distribution of the fragment length *a* on the impact and rear sides. On the impact side, the irradiation did not affect clearly the cumulative number distribution of the maximum length. The fragment from 10 MGy specimen were relatively short. In the case of the unirradiated specimen, the number of fragments over 2 mm was 13 whereas that of fragments from 10 MGy specimen was only 5. On the rear side, the irradiation clearly affected

the cumulative number distribution of the ejecta length. Over a length range from 1 mm to 1.5 mm, the gamma ray irradiation clearly decreased the number of fragments and the fragment size. Only a few fragments which maximum length was 2.2 mm were collected from 10 MGy specimen. It seems to be difficult for 10 MGy specimen to form large fragments.

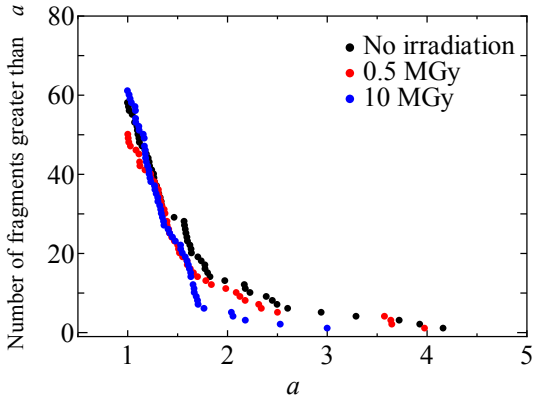

(a) Front side

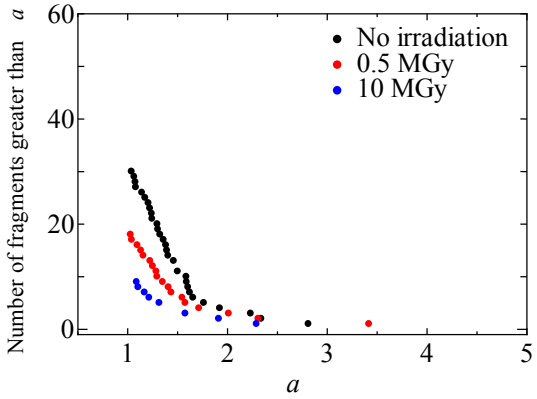

(b) Rear side

Figure 5. Size distribution of ejecta length, 2.4 km/s.

Fig. 6 shows photographs of witness plates after impact tests. On the impact side, a few craters impacted by fragments were observed. On the rear side, we can see many small craters impacted by fragments in the case of the unirradiated specimen and 0.5 MGy specimen. 10 MGy specimens showed a large crater because the projectile struck on the rear witness plate without being fragmented. We can see only a few minuscule craters.

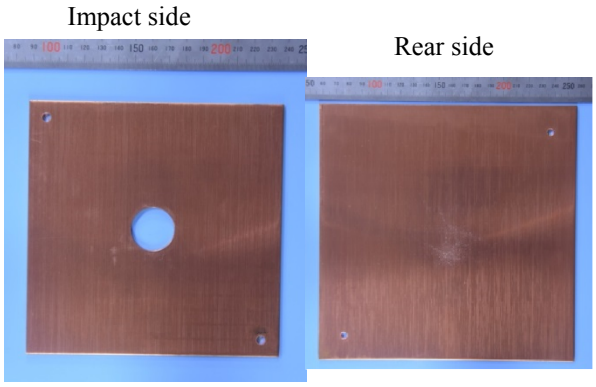

(a) No irradiation (2.41 km/s)

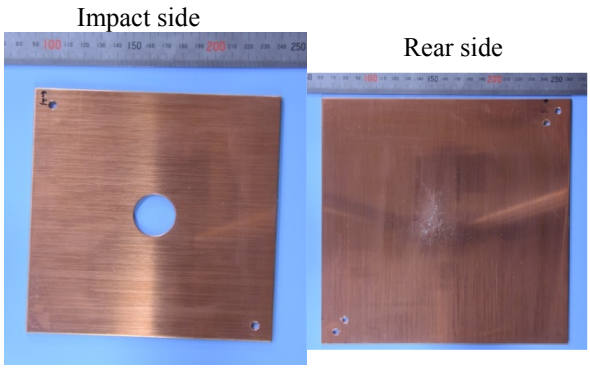

(b) 0.5 MGy (2.38 km/s)

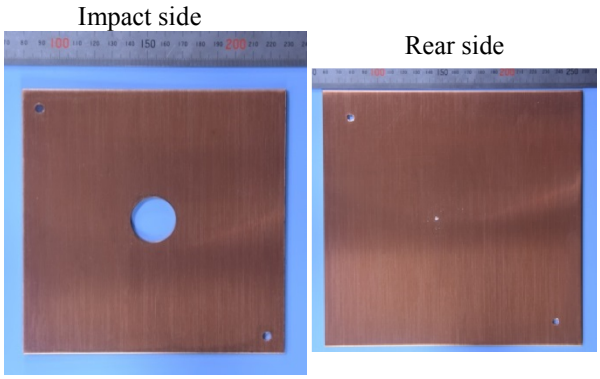

(c) 10 MGy (2.41 km/s)

Figure 6. Photographs of witness plates after impact experiments

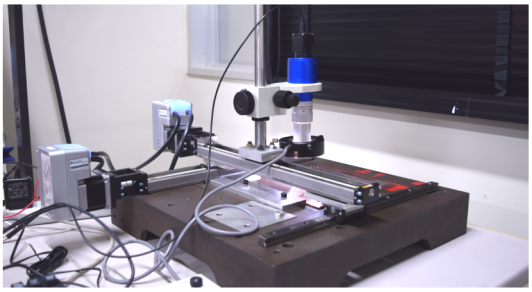

Figure 7. Photographs of scan system

Enlarged images of witness plates were taken by a scan system using a microscope (Saitoh Kogaku, SKM-Z200C-PC) as shown in Fig. 7. The diameter and position of impact craters on the witness plates were deciphered by image analysis software, ImageJ based on ISO 11227 [12-14].

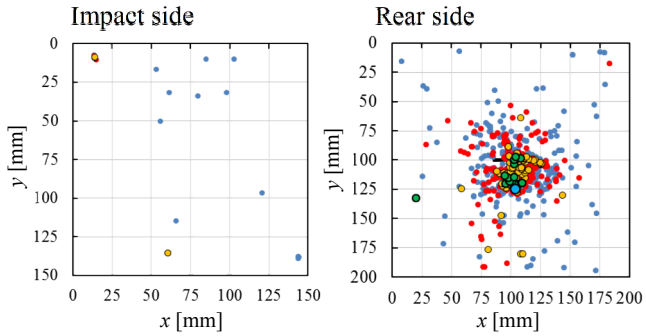

(a) No irradiation (2.41 km/s)

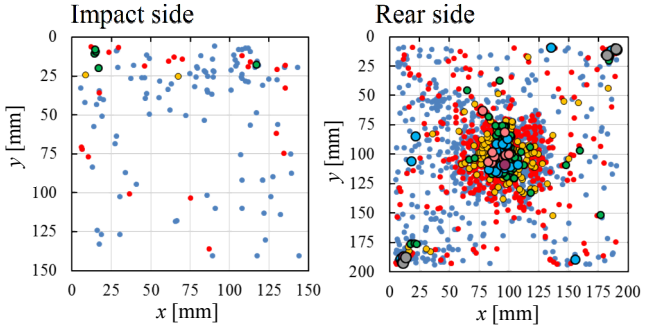

(b) 0.5 MGy (2.38 km/s)

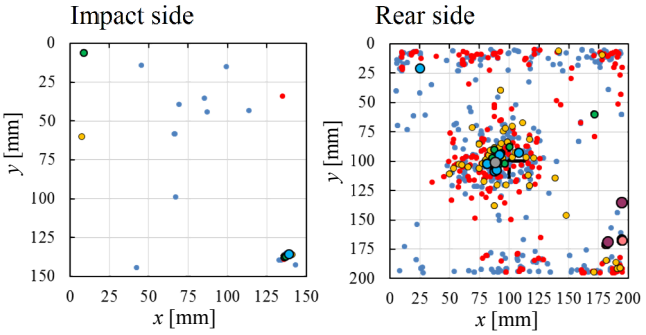

(c) 10 MGy (2.41 km/s)

Figure 8. Photographs of witness plates after impact experiments

Fig. 8 shows analysed results. Fig. 9 shows the meaning of symbols in Fig. 8. On the impact side, a few craters impacted by fragments were observed. There was no clear tendency in three results on impact side. On the rear side, three results show that the crater areas slightly spread from top left to bottom right along to the fiber direction of the outermost layer on the rear side. The spread area from 0.5 MGy specimen was wider than that from the unirradiated specimen. The spread area from 0.5 MGy specimen was wider that the unirradiated specimens and 10 MGy specimen, but the crater number from 0.5 MGy specimen seemed to be higher than that from 10 MGy specimen.

Table 2 shows total number of craters for each size range. As discussed in the section about the observation of witness plate, the three results on impact side shows that a few fragments were scattered. On the rear side, many fragments were scattered. Table 2 shows that the number of craters from 0.5 MGy specimen was clearly higher than those from the unirraeated specimen and 10 MGy specimen.

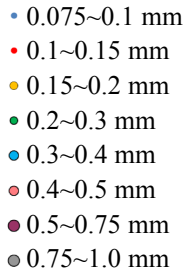

Figure 9. Symbols shown in Fig. 8

Table 2 The number of craters impacted by ejecta

Size range	No irradiation (2.41 km/s)		0.5 MGy (2.38 km/s)		10 MGy (2.41 km/s)	
mm	Impact side	Rear side	Impact side	Rear side	Impact side	Rear side
0.075-0.1	11	1131	108	1196	254	546
0.1-0.15	5	814	28	867	145	331
0.15-0.2	4	212	3	252	26	82
0.2-0.3	0	57	6	111	28	14
0.3-0.4	0	7	0	28	9	14
0.4-0.5	0	1	0	11	0	6
0.5-0.75	0	0	0	3	0	3
0.75-1.0	0	0	0	5	0	1

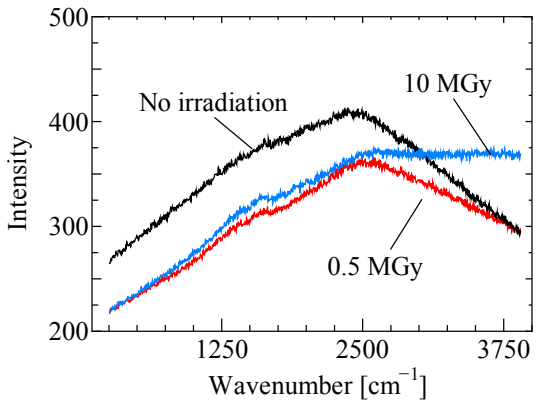

Figure 10. Results of laser Raman spectroscopy

Finally, laser Raman spectroscopy (JASCO, NRS-3300) was applied to the CFRP specimens. A Raman spectrum is shown in Fig. 10. Significant Raman scattering signals were not detected because fluorescence background problems seemed to occur. However, because the trend of fluorescence background was changed by the irradiation (total dose), it is highly possible that some chemical reaction of CFRP such as molecular chain breakage and crosslinking were occurred by the irradiation. Further chemical analyses are needed in order to clarify chemical reaction.

4 CONCLUSIONS

The effects of gamma ray irradiation on fragment size from carbon fiber reinforced plastics (CFRP) plates were examined. On the rear side, the gamma ray irradiation decreased the number of fragments and the fragment size. The penetration hole of projectiles clearly changed with the gamma ray irradiation.

5 ACKNOWLEDGMENTS

This work was supported by JSPS KAKENHI Grant Number JP26420012, Grant-in-Aid for Scientific Research (C). The authors would like to express the deepest appreciation to the financial support from Nagoya Institute of Technology.

6 REFERENCES

1. Barth, J.L., (2003). Space and Atmospheric Environments: From Low Earth Orbits to Deep Space. In *Proc. ICPMSE-6 (Protection of Materials and Structures from Space Environment)* (Eds. Jacob I. Kleiman & Zelina Iskanderova), Kluwer Academic Publishers, USA, pp. 7-29.

2. Grossman, E., Gouzman, I. (2003) Space environment effects on polymers in low earth orbit. *Nuclear Instruments and Methods in Physics Research Section B*. **208**, 48-57.

3. Sasuga, T., Seguchi, T., Sakai, H., Nakakura, T. & Masutani, M. (1989) Electron-beam irradiation effects on mechanical properties of PEEK/CF composite. *J. Mat. Sci.* **24**(5), 1570–1574.

4. Hirade, T., Udagawa, A., Sasuga, T., Seguchi, T. & Hama, Y. (1991). Radiation Effects on Flexural Strength and Mode-I Interlaminar-fracture Toughness of Conventional and Toughened Epoxy Matrix CFRP. *Advanced Composite Materials*. **1**(4), 321-331.

5. Iwata, M., Uchida, J., Kishimoto, N., Higuchi, K. & Goto, K. (2012) Degradation of Carbon Fiber Reinforced Plastics due to Radiation and Prediction of Its End of Life Value on Mechanical Property in Space Radiation Environment, In Proc. 12th International Symposium on Materials in the Space Environment, Noordwijk, The Netherlands.

6. Clegg, R.A., White, D.M., Riedel, W. & Harwick, W. (2006). Hypervelocity Impact Damage Prediction in composites: Part I—Material Model and Characterisation. *Int. J. Impact Eng.* 33(1–12), 190-200.

7. White, D.M., Taylor, E.A. & Clegg, R.A. (2003). Numerical Simulation and Experimental Charcterisation of Direct Hypervelocity Impact on a Spacecraft Hybrid Carbon Fibre/Kevlar Composite Structure. *Int. J. Impact Eng.* 29(1–10), 779-790.

8. Sakuraba, K., Tsuruda, Y., Hanada, T., Liou, J.-C. & Akahoshi, Y. (2008). Investigation and comparison between new satellite impact test results and NASA standard breakup model. *Int. J. Impact Eng.* **35**, 1567–1572.

9. Murakami, J., Hanada, T., Liou, J.-C. & Stansbery, E. (2009). Two new microsatellite impact tests in 2008. *NASA Orbital Debris Quarterly News* **13**, 4.

10. Nishida, M., Kato, H., Hayashi, K. & Higashide, M. (2013). Ejecta Size Distribution Resulting from Hypervelocity Impact of Spherical Projectiles on CFRP Laminates. *Procedia Engineering*, **58**, 533-542.

11. Nishida, M., Kuzuya, K., Hayashi, K. & Hasegawa, S. (2013). Effects of alloy type and heat treatment on ejecta and crater sizes in aluminum alloys subjected to hypervelocity impacts. *Int. J. Impact Eng.* **54**, 161-176.

12. ISO 11227:2012, Space systems -- Test procedure to evaluate spacecraft material ejecta upon hypervelocity impact.

13. Sugahara, K., Aso, K., Akahoshi, Y., Koura, T. & Narumi, T. (2009). Intact Measurement of Fragments in Ejecta Due to Hypervelocity Impact,

In *Proc. 60th International Astronautical Congress*, Curran Associates, Inc., IAC-09-A6.3.06.

14. Nishida, M., Ishida, K., Kodama, F., Hayashi, K., Akahoshi, Y., Hokamoto, K., Mayama, T., Yamasaki, M. & Kawamura, Y. (2017). Lip Formation and Ejecta from LPSO-type Magnesium Alloy Plates in Hypervelocity Impact. *Procedia Engineering*, **173**, 65-72.